

High-throughput nanofluidic device for one-dimensional confined detection of single fluorophores

Siddharth Ghosh,^{*,†,‡} Narain Karedla,[†] and Ingo Gregor[†]

[†]*III. Institute of Physics – Biophysics and Complex Systems, University of Göttingen, 37077 Göttingen, Germany*

[‡]*Current Affiliation: Physics of Light in Complex Systems, Debye Institute for Nanomaterials Science, 3584CC Utrecht, Netherlands.*

E-mail: sghosh@physik3.gwdg.de

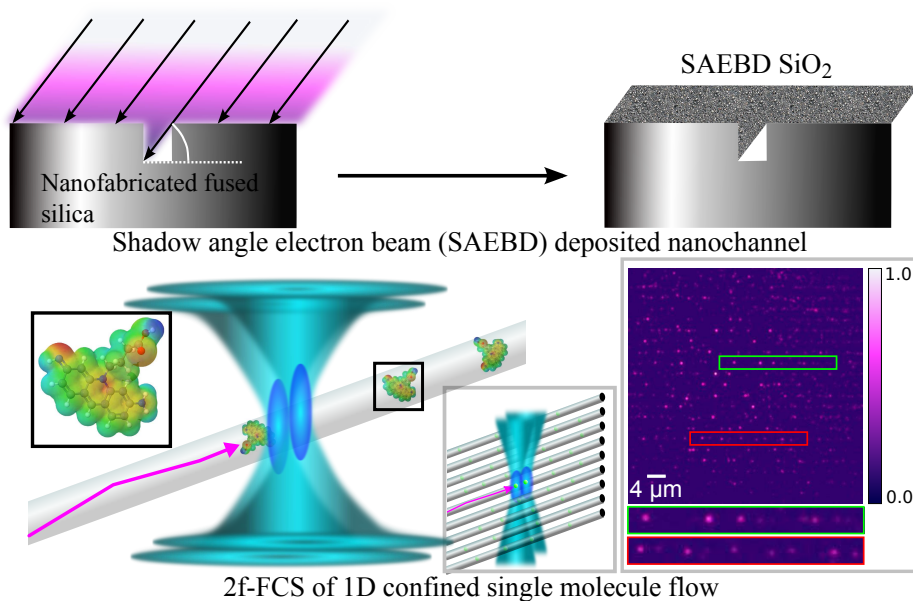
Abstract

Ensemble averaging experiments may conceal many fundamental molecular interactions. To overcome that, a high-throughput detection of single molecules or colloidal nanodots is crucial for biomedical, nanoelectronic, and solid-state applications. One-dimensional (1D) discrete flow of nanoscale objects is an efficient approach in this direction. The development of simple and cost-effective nanofluidic devices is a critical step to realise 1D flow. This letter presents a nanofabrication technique using shadow-angle-electron-beam-deposition for a high-throughput preparation of parallel nanofluidic channels. These were used to flow and detect small fragments of DNA, carbon-nanodots, and organic fluorophores. The 1D molecular mass transport was performed using electro-osmotic flow. The 1D flow behaviour was analysed using two-focus fluorescence correlation spectroscopy (2fFCS). A range of flow velocities of single molecules was achieved – from 15 $\mu\text{m/s}$ to 290 $\mu\text{m/s}$. The transitions of single

molecules or nanodots through the two foci were quantitatively analysed using confocal scanning fluorescence microscopy, correlative photon detection, and burst size distribution analysis. The results suggest an efficient nanofabrication technique is developed to prepare nanofluidic devices. This first demonstration of high-throughput nanochannel fabrication process and using 2fFCS-based single molecule flow detection should have potential impact on ultra-sensitive biomedical diagnostics and studying biomolecular interactions as well as nanomaterials.

Keywords

Nanofluidics, single molecule detection, two-focus fluorescence correlation spectroscopy, photon burst size distribution.



Main text

Due to Brownian motion, it is impossible to keep a molecule within the detection volume for an extended period of time. The study of nanofluidics became popular to circumvent this problem with wide scientific applications.¹⁻⁴ With the advancement of nanotechnologies,

nanofluidic devices comprising arrays of nanochannels with diameters less than hundred nanometres have become significant for bioanalytical diagnostics applications, such as DNA optical mapping,⁵⁻⁸ single virus and nanoparticle detection.⁹⁻¹⁴ Nanochannels are useful tools allowing systematic studies of entities from single molecule to viruses over long periods of time. It can induce 1D fluidic confinement by suppressing the thermal motions in two directions.

The primary problem is to establish a simple and efficient way of nanofabricating 1D nanofluidic channels. Different methods have been published, which described the fabrication processes of such nanofluidic devices.¹⁸⁻²² However, majority of them are technically challenging, costly, and not easily applicable for high-throughput production. Hence, we present a cost-effective and simple nanofabrication technique based on electron beam lithography (EBL) and shadow-angle-electron-beam-deposition (SAEBD).

The nanochannels were used to detect a flow of photoluminescent nanomaterials, such as small DNA molecules labelled with single organic fluorophores, carbon nanodots (CND),²³ and pure organic fluorophores. Using two-focus fluorescence correlation spectroscopy (2fFCS),²⁴⁻²⁷ we recorded the transits of single molecules or nanodots through the nanochannels, and quantitatively analysed their flow velocities. Here, the detection regions were two diffraction limited focal spots with a lateral displacement of 400 nm. To ensure 1D transport between the two foci, the diameter of the nanochannels should be smaller than the focal diameters. The nanochannels presented here have diameters ranging from 30 nm to 100 nm, which are smaller than the focal diameter.

The process steps to create an enclosed nanochannels involve – nanofabrication of open nanochannels using EBL and RIE and enclosing them using SAEBD. The ballistic path of the electron beam (e-beam) assisted evaporation²⁸ is the principle behind SAEBD. When a straight beam of depositing material hits onto an open nano-trench at shallow incident angles, no deposition occurs in the shadowed region.^{29,30} Such deposition can enclose a large number of parallel nanochannels (depending on the e-beam diameter) leaving the shadowed

region as the fluidic path of interest. The process is unaffected by nanometre sized leftover residues of the e-beam resists and does not require an atomically clean surface, unlike any wafer bonding process.³¹ For optical reasons, the final nanochannels were prepared using pure silicon dioxide. Being an insulator silica contributes to surface charging under e-beam which affects EBL and SEM. EBL and SEM induced surface charges were compensated using a thin-film of gold. Here we show the SAEBD process using silicon to obtain high resolution electron microscopy images of the intermediate steps.

Figure 1a shows a schematic flow-chart of creating nanochannels on [100] silicon wafers. The width of the nano-trenches (i.e. the final width of the enclosed nanochannels) can be optimised by the e-beam exposure of the EBL to the positive e-beam resist. Different widths of nano-trenches were created ranging from 30 nm to 100 nm. In Figure 1b we observe nano-trenches of such widths, 65 nm and 100 nm. The nanolithographed e-beam resist acted as a mask for RIE to etch the final nano-trenches on silicon. The depth of the nano-trenches was investigated with AFM as 35 nm to 40 nm.

In the next step, SAEBD was used to enclose the nano-trenches to create enclosed nanochannels. Figure 1c schematically explains the concept of the SAEBD process. A high-energy e-beam (bent with magnet) sublimates the material which deposits onto the substrate. Figure 1d schematically explains the role of deposition angle (θ). The shadowed region is created due to the angular depositions. This region is unexposed to the depositing material. The deposited region and shadowed region are colour coded red and yellow, respectively. In the time evolution schematic, the SAEBD leads to enclosing the nano-trenches leaving apart a void. By decreasing θ , one can increase the hypotenuse. At an acute angle close to 0° , the hypotenuse becomes nearly parallel to the base as shown in Figure 1e-h. Figure 1e schematically represents a high angle deposition which was realised at 80° in Figure 1f. Here, an array of 5 mm long nano-trenches were cross-sectioned using a wafer sawing instrument to observe the intermediate steps while performing SAEBD. Figure 1g schematically represents a low angle deposition which was realised at 45° in Figure 1f. Designing the

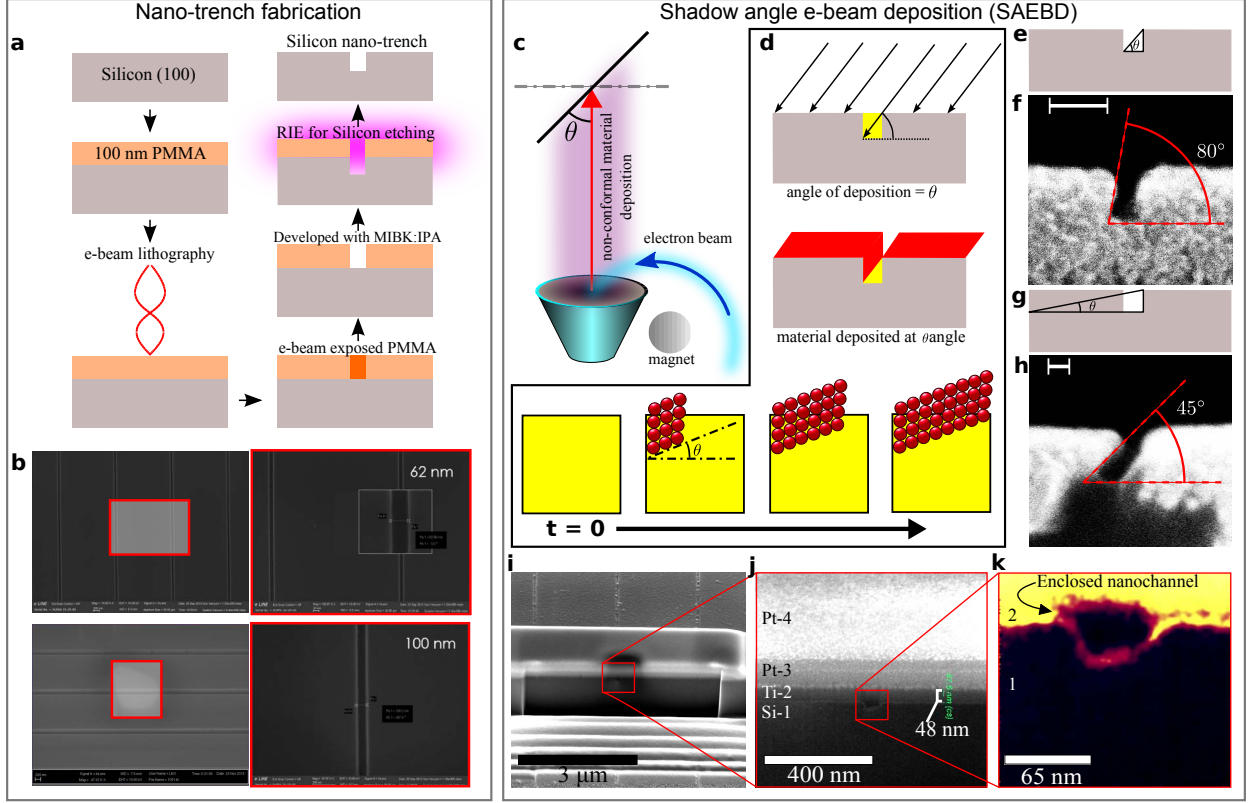


Figure 1: **Nanochannel fabrication using SAEBD.** **a.** Fabrication of nano-trenches on silicon with EBL and RIE. **b.** SEM of silicon nano-trenches with 62 nm and 100 nm width. **c.** SAEBD at angle θ . **d.** Shadows of electron beam – arrows represent angular e-beam evaporation. **e.** Schematic of high angle deposition and **f.** SEM of deposition at 80° . **g.** Schematic of low angle deposition and **h.** SEM of deposition at 45° . **i.** FIB cross-section of the enclosed nanochannels. Two layers of platinum were used to protect the nanochannel from high energy ions. **j.** Magnified view of the enclosed nanochannel, where Si-1 is the silicon substrate on which nano-trenches were fabricated, Ti-2 is the 50 nm thick titanium layer which was used in SAEBD, Pt-3 and Pt-4 were platinum deposited inside FIB. **k.** Further magnified view of the nanochannel where '1' represent silicon (Si-1) and '2' represent titanium (Ti-2).

deposition stage is difficult for an acute angle close to 0° . Nevertheless, satisfactory results were obtained using $\theta = 45^\circ$ as shown in Figure 1i-k. 60 nm titanium was deposited on the open nano-trenches at an angle of 45° with a deposition rate of $1\text{\AA}/\text{s}$ at a pressure of 2×10^{-6} mbar. We predict that at an angle 30° one can prepare high-quality flat edge.

We used FIB to cross-section the produced nanochannels for characterisation. To avoid ion beam induced damage, the top part of the region to be milled was protected with metallic thin-film layers. We deposited two thin-films on the top surface of the enclosed nanochannels.

Figure 1*i* - *k* show SEM images of the milled regions from low to high magnification. In Figure 1*j* the first layer (Si-1) is the silicon substrate on which nano-trenches were fabricated. The second layer is the 45° SAEBD-ed titanium (Ti-2) layer. The third and fourth layers – Pt-3 and Pt-4 are platinum layers of 100 nm and 450 nm, respectively – acted as protective layers to avoid FIB induced damage. Pt-3 and Pt-4 were deposited using FIB, which have no relation to the SAEBD process. In Figure 1*k*, we observe the magnified cross-section of an enclosed nanochannel. Here, ‘1’ and ‘2’ refer to Si-1 and Ti-2 layers, respectively. As speculated, the non-conformal SAEBD growth of titanium thin-film produces a well defined flat encloser of the nanochannel. A 60 nm of titanium SAEBD at 45° angle should produce a vertical thickness of 51 nm. In Figure 1*j*, the vertical thickness of the titanium film is 47.8 nm. Considering the uncertainty of few nanometres deposition thickness, this agrees well with our expectation.

After this proof of principle experiment with titanium, fused silica based nanofluidic devices were prepared. Here, 5 nm of gold thin-film was sputter coated prior to spin-coating e-beam resist on the silica wafer. Monte-Carlo simulations were performed to optimise gold thin-film thickness in order to reduce charging effect of silica under EBL. Fused silica based nano-trenches were enclosed with SAEBD using silicon dioxide at 45°.

The design of the silica based nanofluidic device to perform single molecule experiments is schematically illustrated in Figure 2*a*. It has two reservoirs with gradual decrease of length-scale from milli-scale to microscale and finally, the nanometre-sized channels. Two milli-scale reservoirs were used as inlet and outlet. These two inlets were sand blasted on silica wafers using 70 μm silica particles prior to nanofabrication process. The microscale reservoirs with the same thickness of nanochannels and micrometre width were etched with RIE. In the Figure 2*a*, the white regions and blue regions are milli-scale and microscale reservoirs, respectively (Supporting information Figure S1 and S2). The red stripes correspond to nanochannels. They are connected to the microscale reservoirs. An SEM image of these silica nanochannels is also shown in the right inset of Figure 2*a*. We filled these nanochannels

with a solution of fluorescent probes. They were unidirectionally transported with electro-osmotic flow^{32–35} as shown in Figure 2b. After filling one reservoir with fluorescent molecules (diluted in PBS buffer - see methods - electro-osmotic flow) capillary force transported the fluid to the other reservoir. A relaxation time of 30 s was given to avoid development of trapped air bubbles, and then only, the second reservoir was filled. Two 100 μm thick platinum electrodes were immersed into the PBS filled reservoirs (supporting information Figure S1), and an electric field was applied along the nanochannel (supporting information Figure S1 and S4 – electrode integration with the nanofluidic device). In Figure 2c, single Alexa-647 fluorophore molecules (purchased from Thermo Fisher, Massachusetts, USA) are horizontally lined up in all the parallel nanochannels. The pixel to photon counts profile plot shows an average SNR of 90. This image was captured with a wide-field optical microscope by exciting the molecules with a 640 nm continuous wave laser (Coherent Laser Systems GmbH, Göttingen, Germany). Beside the evidence of FIB and SEM, this also infers that the nanochannels are properly enclosed. No cross-talking of single molecules is observed among nanochannels.³¹

Fluid flow inside a nanochannel is 1D when $D_f \gg d_{nc}$, where D_f and d_{nc} are the diameters of the detecting region and the nanochannels, respectively (Figure 2a). The degree of confinement is acceptable until the molecule is forced within the detection volume. This condition is satisfied because in our case D_f is 300 nm to 500 nm (excitation wavelength dependent) and d_{nc} is 30 nm to 100 nm.

The in-time and out-time of flowing single molecules within detection volumes were correlated using two APDs of 2fFCS (Figure 2b).²⁵ The diffraction limited two foci of 2fFCS were 40 MHz pulsed interleaved excitation. The two foci were partially overlapping with each other. They were generated using a Nomarski prism, a $100\times$ 1.49 NA of oil immersion objective, and two linearly polarised lasers perpendicular to each other. An x - y - z piezo-scanner was used to acquire scan images and point measurements of photon counts.

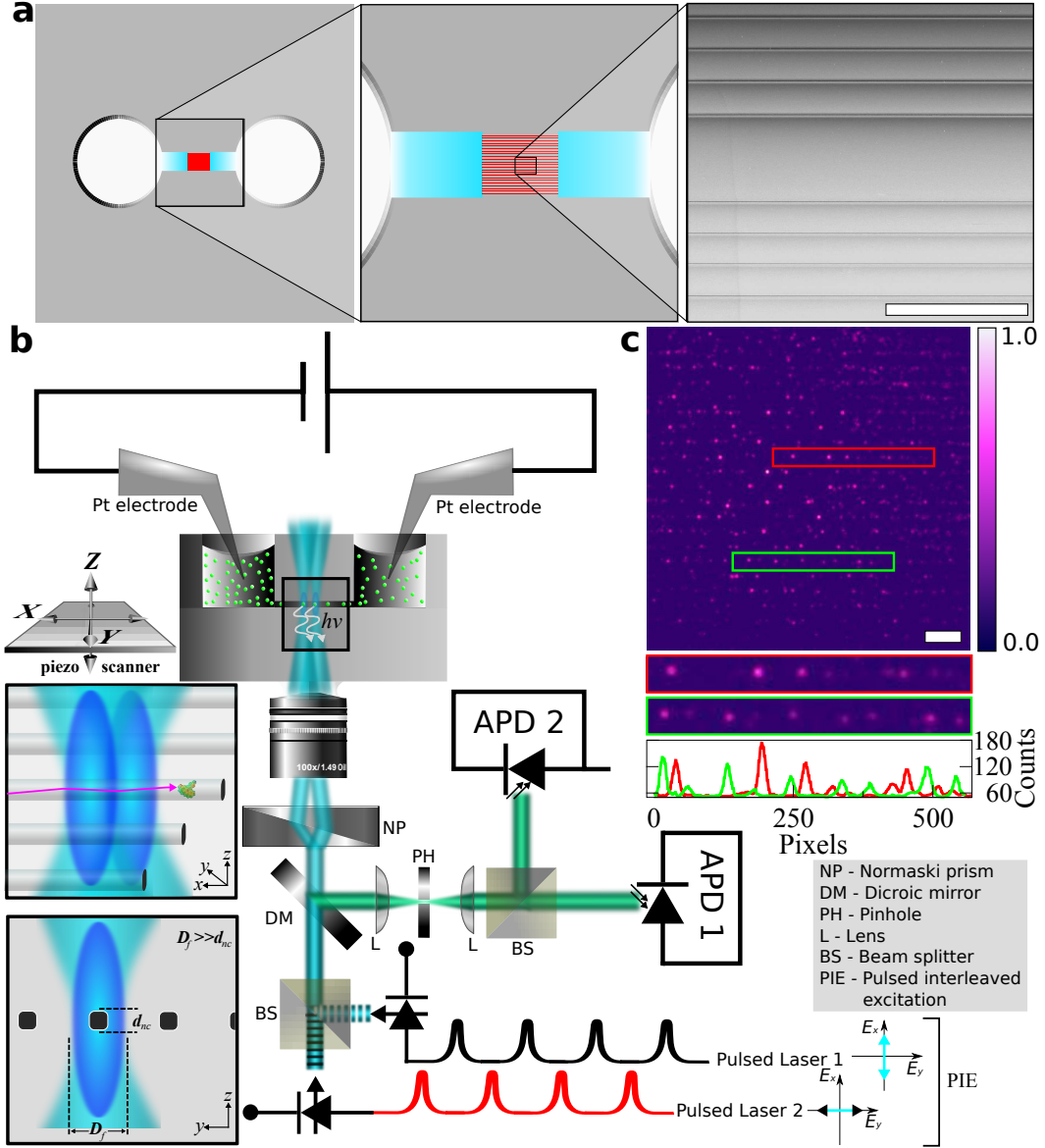


Figure 2: **Nanofluidic device in a 2fFCS setup.** **a.** Schematic top view of nanofluidic device together with an SEM image of real nanochannels (scale bar is 30 μm). **b.** Side view schematic of the complete experimental set up where electric field is applied through two reservoirs along the nanochannels using platinum electrodes. Two foci (of 2fFCS) were aligned with nanochannel using a 100 \times 1.49 NA oil immersion objective lens. Two different linearly polarised pulsed interleaved lasers were used for in two foci – excitation. The emission from flowing single molecules was detected with two APDs. **c.** A wide-field of image frame showing the presence of single molecule (scale bar is 8 μm).

To restrict unwanted surface adsorption of single molecule, we used fluorescent molecules carrying the same charge as the nanochannels' wall. Pure silica is negatively charged above its

isoelectric point ($\text{pH(I)} = 2$).^{36,37} A buffer of pH 8.5 was used to increase the negative charges on the walls of silica nanochannels. The condition was suitable to flow negatively charged molecules without being adsorbed. We chose carbon-nanodots (CND) as the first probe of interest. They are <2 nm in size²³ and negatively charged (see supporting information Figure S5). A confocal scanned image was recorded along the x - y plane when CNDs were flowing inside nanochannel. In the schematic top-view of the nanochannels in Figure 3a – dark lines are the nanochannels. They were filled with carbon-dots (Figure 3b). The pixel size (p_a) of the image is 320 nm with dwell time (δt) of 5 ms. To record this focused z plane in Figure 3b, we performed a y - z scanned image and went to the position, where the count-rate was maximum. The scheme of y - z piezo-scan is shown in Figure 3c. The height-wise cross-section of several periodic point spread functions (PSF) were recorded from periodic nanochannels. When single CNDs are flowing in unidirectionally, jittery (or fluctuating) fluorescent signals are recorded as observed in the periodic PSFs – Figure 3d, e, and f. An ascending concentrations of aqueous CND solutions were used. In Figure 3d to g, the volume percentage of CNDs in water relative to its stock solution are 1%, 2%, 5%, and 50%, respectively. Here, p_a is 100 nm and δt is 2 ms. The applied electric field to induce electro-osmotic flow during the measurement was 15 V/mm. As the concentration of CNDs increased, the fluctuations of the photon signal decreased due to increasing rate of CNDs arrival in the focal volume (Figure 3d - g).

Time-correlated analysis of photon counts was carried out to investigate flow velocities of single molecules. These measurements were carried out at the highest photon counted points of y - z scanned PSFs. Prior to performing every 2fFCS measurement, a y - z scan was taken as shown in Figure 4. To substantiate that our method is not restricted to a particular fluorescent probe, we performed 2fFCS of Atto 488 dye (see supporting information for a control measurement of diffusion Figure S6) and 48 base-pair of DNA labelled with single Alexa-647 fluorophore (purchased from IBA GmbH, Göttingen, Germany). The electrolytic aqueous buffer solution used for the electroosmotic flow is detailed in the Method section.

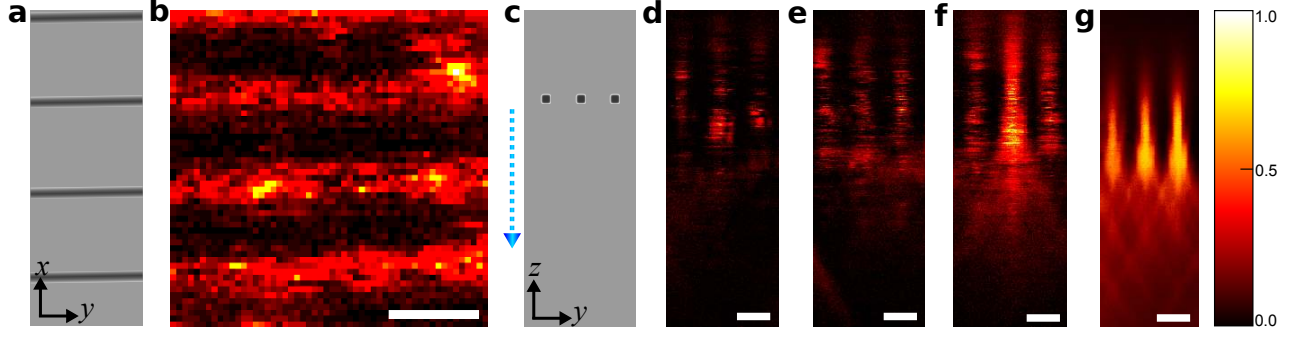


Figure 3: **1D Flow of CNDs.** **a.** Schematic top-view of nanochannels along which an (y - x) scan was performed. **b.** Confocal scan image of nanochannels filled with CNDs. **c.** Schematic cross-sectional side view of nanochannels along which (y - z) scans were performed. The dashed arrow represent the optical excitation path – direction from immersion oil of objective lens to nanofluidic device. **d.**, **e.**, and **f.** y - z scan images of nanochannels with an increasing order of CNDs' concentration flowing through nanochannels. **g.** High concentration of CND. All the horizontal scale bars denotes 2 μm . The vertical scale bar denotes photon counts as 0.0 (lowest) to 1.0 (highest).

We measured the flow velocities of single DNA molecules inside 1D nanochannel within a range of applied electric field from 27 V/mm to 300 V/mm (see supporting information Figure S7). These measurements were performed inside a nanochannel with d_{nc} of 30 nm. The correlated photon counts provide two autocorrelations for two foci, and one forward and one backward cross-correlation between them.^{26,27} A difference should be observed in two cross-correlations due to a unidirectional flow profile as shown earlier by Arbour and Enderlein.²⁷ The correlated data points from 2fFCS are fitted with the Fokker-Planck equation³⁸ considering the 1D electro-osmotic flow.

An exemplary correlated photon counts of 1D flow measurement performed at 220 V/mm is shown in Figure 4a. Here, sky-blue and red fitted curves are two cross-correlations, and other two curves are autocorrelations. The velocity and diffusion coefficient from the curve fitting are $1.51 \times 10^{-7} \text{ cm}^2/\text{s}$ and $-207 \text{ }\mu\text{m}/\text{s}$, respectively. The negative value of the flow velocity infers the direction of the flow, which can be altered by changing the applied polarity of the electric field. The linear relationship of electro-osmotic flows at different applied electric fields is plotted in Figure 4b. The linear fit has an r^2 value of 0.992.

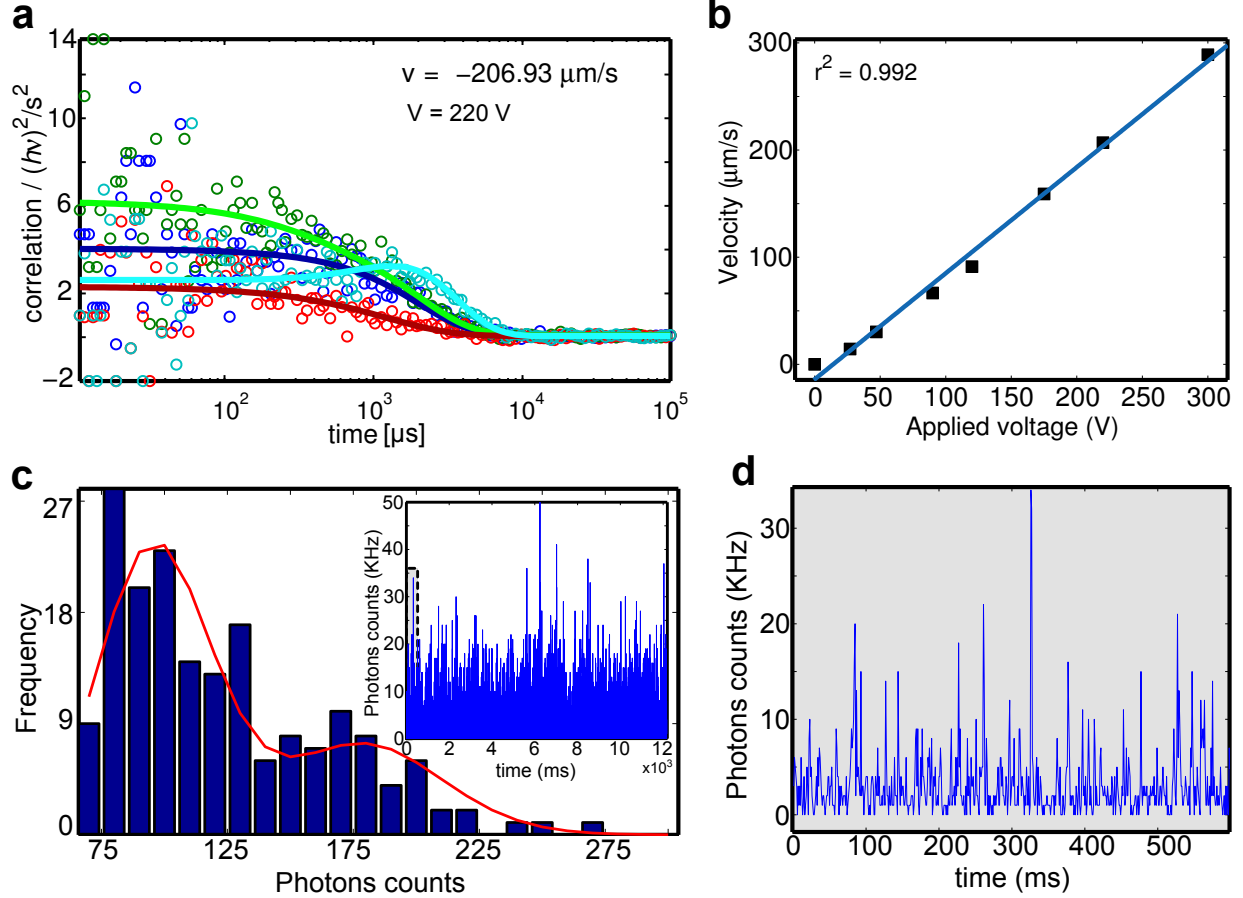


Figure 4: 1D Flow of 48bp DNA. **a.** 2fFCS measured correlation plots of photon counts from two APDs. Here, applied electric field was of 220 V/mm. The data was fitted with 1D Fokker-Planck equation. From the fitting, we found diffusion coefficient of $1.51 \times 10^{-7} \text{ cm}^2/\text{s}$. **b.** Plot of velocity versus applied voltage along the nanochannel. The data was fitted with linear fit. **c.** Burst size distribution of single molecule transits fitted with two Poissonian distributions. Total time trace binned with 5 ms is shown in the inset. The inset showing total time trace – the dashed bordered grey region is shown in **d.** **d.** A part of the time trace plots of single photon bursts due single DNA molecules transits through focus.

To confirm whether the photon used in 2fFCS were from aggregates of single molecules, photon burst sizes of molecular transits were analysed.³⁹ Burst size distribution (BSD) of the complete time trace for a flow measurement is shown in Figure 4c. The complete time trace used in the BSD analysis is shown in the inset. We fit the BSD with Poisson distributions. The first peak is due to the single molecule bursts, and the second is due to multiple-molecule-events as observed by Enderlein et al.³⁹ Multiple-molecule-events occur when more

than one molecule transits through focus in close succession that the detectors cannot resolve the temporal discretisations between two or more molecules. Figure 4d shows a magnified region of the inset 5 ms binned time-trace of Figure 4c where 0 to 600 ms is highlighted with a dashed box (grey inside). We clearly observe single molecule bursts in Figure 4d.

In summary, this letter presented an efficient method (SAEBD) of nanofabricating nanochannels and their usage in single molecule nanofluidics to confine the thermal fluctuations. The nanofabrication process demonstrated here is simple and high-throughput for large scale production of nanofluidic chips. The process is not material restricted, unlike the oxidation and bonding based techniques. Single fluorophore molecules, CNDs, and DNA molecules were studied inside nanochannels. 1D flows of them inside nanochannel were achieved using electro-osmosis. Wide-field and confocal microscopy were used for qualitative analysis of the 1D flow. Using 2fFCS method the 1D flows of the mentioned species were quantitatively analysed. A broad range of velocities was observed by varying the applied electric field along the nanochannels. The BSD analysis confirm that the observed transits were mainly due to single emitters. All the experiments were performed inside nanochannels of $30\text{ nm} \times 35\text{ nm}$ in cross-section. This simple and high-throughput approach of fabricating nanochannels paves the way towards detecting early onset of any disease at single molecule level. In future, trapping nanoscale objects of less than 2 nm in size for large residence time should be also feasible using these nanochannels. Biomolecular interactions such as dynamics of DNA, protein aggregation, and structural biology of molecules in physiological condition can be also studied at single molecule level using the SAEBD based nanofluidic devices.

Methods

Nanofabrication: A rigorous cleaning of the surface of interest is required to eliminate unwanted organic or dust-particle contaminations. The silicon wafers were ultrasonicated with acetone prior to piranha cleaning at 120° C for 15 min. The piranha cleaned wafers were then rinsed with de-ionised water. The wafers were heated at 180° C for 10 min

to make sure all the water molecules were evaporated. The cleaning protocol was carried out inside a class 100 cleanroom. Prior to spin-coating, the wafers with e-beam resist, an upright optical microscope with 100 \times objective lens was used to investigate the surface of the silicon. Fused silica wafers were cleaned with RCA1 reagents instead of piranha. The pristine wafers were spin-coated with the e-beam resist PMMA-A2 (polymethylene methacrylate from MicroChem Corp., Newton, United States) at 2000 rpm for 60 s. The spin-coated wafers were then baked at 180 $^{\circ}$ C for 90 s. A uniform 100 nm thick PMMA film was produced on the wafers. EBL was carried out on the PMMA coated wafers using fixed-e-beam-moving-stage condition⁴⁰ The first experiment where silicon wafers were used – nanochannel dimensions were 2 mm long and 30 nm - 100 nm wide. The final fused silica based nanofluidic device contained 100 – 150 μ m long nanochannels. To avoid overlapping periodic PSFs, the distance between every two nanochannels was 2 – 3 μ m. The EBL exposed PMMA was monomerised and removed by immersing the wafers into MIBK:IPA (methyl isobutyl ketone dissolved in isopropanol purchased from MicroChem Corp., Newton, United States) developer at -20 $^{\circ}$ C for 30 s. After 30 s, the wafers were immersed into isopropanol to stop over-development and nitrogen blown dried. Nanometre scale openings were formed revealing the silicon or silica where PMMA was removed with the developer. The remaining undeveloped PMMA regions acted as a mask where no etching was performed for RIE. The reactive plasma was created at high vacuum.

This process-flow is schematically described in Figure 1a. After the RIE treatment, the left-over PMMA (mask-region) was removed with acetone, piranha, and oxygen RIE.

SAEBD: SAEBD was performed using a Leybold Univex 350 e-beam evaporation system purchased from Oerlikon Leybold Vacuum GmbH, Cologne, Germany. The vacuum pressure inside the chamber while evaporation was 1×10^{-6} mbar. The dicing system used to cross-section the silicon wafers was Disco Dad 320 purchased from Disco Corporation, Tokyo, Japan. The diamond blade used in the system was ZH05-SD2000-N1-70 (Disco Corporation, Tokyo, Japan).

FIB: FIB used here is Nova NanoLab 600 DualBeam purchased from FEI Company, Hillsboro, USA. The protection layer of platinum was deposited in two separate growth rates. At the interface of Ti-2 we used 1 pA current for the deposition to achieve an uninterrupted and atomic interface. The top most surface (Pt-4) was grown at fast deposition rate because this surface is the first interacting surface with FIB dissipating majority of the damaging ionic bombardments. To avoid any damage at the region of interest, ion beam was created with 1 pA current at system vacuum of 1.5×10^{-6} mbar.

2fFCS setup: We used the commercial confocal system Microtime 200 (PicoQuant, Berlin, Germany) for scanning our samples and performing 2fFCS. The details of the setup are included in the supporting information.

Buffer: Electro-osmotic flow was performed using 300 pM of 48 base-paired DNA (11 nm long) tagged with Alexa647 was diluted with Tris Buffer and 30%Glycerol with pH of 8.5.

Supporting Information

The supporting information contains the description of integrating the nanochannels to electrodes, design of the nanofluidic device, carbon nanodots cation-pi interaction behaviour, 2fFCS measured 1D diffusion of single Atto 488 fluorophores and electro-osmotic flow of single DNA molecules at different electric fields.

Acknowledgement

S.G. thanks the International Max Planck Research School for Physics of Biological and Complex Systems and the Ministry of Science and Culture (Lower Saxony) for awarding an Excellence Stipend/MWK Ph.D. scholarship. The work presented here was carried out at the research group of Prof. Jörg Enderlein. The authors thank the internal funding from the University of Göttingen associated to the Third Institute of Physics for this project. Lastly, the authors are extremely grateful to Prof. Enderlein for providing enormous amount of

critical scientific advices.

Authors Contribution

S.G. has written the manuscript, conceptualised the idea of nanofabrication, prepared the nanofluidic device, performed all the measurements and numerical fitting presented in this paper. S.G. and N.K. have performed initial measurements together (not presented here). N.K. have modified the fitting routine provided by Prof. Jörg Enderlein and I.G. I.G. has supervised the project and provided all necessary scientific advices. All the authors have read and made adequate correction in the manuscripts.

References

- (1) Jan CT Eijkel, and Albert Van Den Berg. *Nanofluidics: what is it and what can we expect from it?* Microfluidics and Nanofluidics 1, no. 3 (2005): 249-267.
- (2) Sumita Pennathur, and Juan G. Santiago. *Electrokinetic transport in nanochannels. 1. Theory.* Analytical Chemistry 77, no. 21 (2005): 6772-6781.
- (3) Miao Wang, Nan Jing, Chin B. Su, Jun Kameoka, Chao-Kai Chou, Mien-Chie Hung, and Kuang-An Chang. *Electrospinning of silica nanochannels for single molecule detection.* Applied physics letters 88, no. 3 (2006): 033106.
- (4) Prakash Goswami, and Suman Chakraborty. *Energy transfer through streaming effects in time-periodic pressure-driven nanochannel flows with interfacial slip.* Langmuir 26, no. 1 (2009): 581-590.
- (5) Fredrik Persson, and Jonas O Tegenfeldt, *DNA in Nanochannels—Directly Visualizing Genomic Information.* Chemical Society Reviews 39 (2010): 985-999.

- (6) Seung Kyu Min, Woo Youn Kim, Yeonchoo Cho, and Kwang S. Kim. *Fast DNA sequencing with a graphene-based nanochannel device*. Nature Nanotechnology 6, no. 3 (2011): 162-165.
- (7) Bala Murali Venkatesan and Rashid Bashir. *Nanopore sensors for nucleic acid analysis*. Nature Nanotechnology 6, no. 10 (2011): 615-624.
- (8) Chao Wang, Robert L. Bruce, Elizabeth A. Duch, Jyotica V. Patel, Joshua T. Smith, Yann Astier, Benjamin H. Wunsch et al. *Hydrodynamics of diamond-shaped gradient nanopillar arrays for effective DNA translocation into nanochannels*. ACS nano 9, no. 2 (2015): 1206-1218.
- (9) Anirban Mitra, Bradley Deutsch, Filipp Ignatovich, Carrie Dykes, and Lukas Novotny. *Nano-optofluidic detection of single viruses and nanoparticles*. ACS nano 4, no. 3 (2010): 1305-1312.
- (10) Mark N. Hamblin, Jie Xuan, Daniel Maynes, H. Dennis Tolley, David M. Belnap, Adam T. Woolley, Milton L. Lee, and Aaron R. Hawkins. *Selective trapping and concentration of nanoparticles and viruses in dual-height nanofluidic channels*. Lab on a Chip 10, no. 2 (2010): 173-178.
- (11) Jean-Luc Fraikin,, Tambet Teesalu, Christopher M. McKenney, Erkki Ruoslahti, and Andrew N. Cleland. *A high-throughput label-free nanoparticle analyser*. Nature nanotechnology 6, no. 5 (2011): 308-313.
- (12) Alfredo de la Escosura-Muniz, and Arben Merkoci. *A Nanochannel/Nanoparticle-Based Filtering and Sensing Platform for Direct Detection of a Cancer Biomarker in Blood*. Small 7, no. 5 (2011): 675-682.
- (13) Sanli Faez, et al. *Fast, label-free tracking of single viruses and weakly scattering nanoparticles in a nanofluidic optical fiber*. ACS nano 9.12 (2015): 12349-12357.

- (14) Sanli Faez, et al. *Nanocapillary Electrokinetic Tracking for Monitoring Charge Fluctuations on a Single Nanoparticle*. Faraday Discussions (2016).
- (15) Adam E. Cohen *Trapping and manipulating single molecules in solution*. Diss. Stanford University, 2006.
- (16) Manoj Kumbakhar, Dirk Hähnel, Ingo Gregor, and Jörg Enderlein. *Feedback-controlled electro-kinetic traps for single-molecule spectroscopy*. Pramana 82, no. 1 (2014): 121-134.
- (17) Marco Braun, Andreas Paul Bregulla, Katrin Guenther, Michael Mertig, and Frank Cichos. *Single Molecules Trapped by Dynamic Inhomogeneous Temperature Fields*. Nano letters (2015).
- (18) Fredrik Persson, L H Thamdrup, M BL Mikkelsen, S E Jaarlgar, P Skafte-Pedersen, H Bruus, and A Kristensen, *Double thermal oxidation scheme for the fabrication of SiO₂ nanochannels*. Nanotechnology 18 (2007): 245301-245305.
- (19) Daniel C S Bien, Hing Wah Lee and Rahimah Mohd Saman, *Fabrication of High aspect ratio silicon nanochannels arrays*. ECS Solid State Letters1 (2012): 45-47.
- (20) So Hyun Kim, Yidan Cui, Min Jung Lee, Seong-Won Nam, Doori Oh, Seong Ho Kang, Youn Sang Kim and Sungsu Park, *Simple fabrication of hydrophilic nanochannels sing the chemical bonding between activatied ultrathin PDMS layer and cover glass by oxygen plasma*. Lab Chip 11 (2011): 348-353.
- (21) Fredrik Westerlund, Fredrik Persson, Anders Kristensenb and Jonas O. Tegenfeldt, *Fluorescence enhancement of single DNA molecules confined in Si/SiO₂ nanochannels* Lab Chip 10 (2010): 2049.
- (22) Pan Mao and Jongyoon Han, *Fabrication and characterization of 20 nm planar nanofluidic channels by glass-glass and glass-silicon bonding*. Lab Chip 5 (2005): 837-8.

- (23) Siddharth Ghosh, Anna M. Chizhik, Narain Karedla, Mariia O. Dekaliuk, Ingo Gregor, Henning Schuhmann, Michael Seibt et al. *Photoluminescence of Carbon Nanodots: Dipole Emission Centers and Electron-Phonon Coupling*. Nano letters 14, no. 10 (2014): 5656-5661.
- (24) Michael Brinkmeier, Klaus Dörre, Jens Stephan, and Manfred Eigen. *Two-beam cross-correlation: a method to characterize transport phenomena in micrometer-sized structures*. Analytical chemistry 71, no. 3 (1999): 609-616.
- (25) Thomas Dertinger, Victor Pacheco, Iris von der Hocht, Rudolf Hartmann, Ingo Gregor, and Jörg Enderlein. *Two-focus fluorescence correlation spectroscopy: A new tool for accurate and absolute diffusion measurements*. ChemPhysChem 8, no. 3 (2007): 433-443.
- (26) Thomas Dertinger, Anastasia Loman, Benjamin Ewers, Claus B. Moeller, Benedikt Kraemer, and Jörg Enderlein. *The optics and performance of dual-focus fluorescence correlation spectroscopy*. Optics express 16, no. 19 (2008): 14353-14368.
- (27) Tyler J. Arbour, and Jörg Enderlein. *Application of dual-focus fluorescence correlation spectroscopy to microfluidic flow-velocity measurement*. Lab on a Chip 10, no. 10 (2010): 1286-1292.
- (28) J. J. Merkel, T. Sontheimer, B. Rech and C. Becker. *Directional growth and crystallization of silicon thin films prepared by electron-beam evaporation on oblique and textured surfaces*. Journal of Crystal Growth 367 (2013): 126-130.
- (29) Stefan Egger, Adelina Ilie, Shinichi Machida, and Tomonobu Nakayama. *Integration of individual nanoscale structures into devices using dynamic nanostenciling*. Nano letters 7, no. 11 (2007): 3399-3404.
- (30) Mattox, Donald M. *Handbook of physical vapor deposition (PVD) processing*. William Andrew, 2010.

- (31) Siddharth Ghosh, Manoj Kumbhakar, Mitja Platen, Ingo Gregor, and Jörg Enderlein. *Single-molecule fluorescence inside solid-state nanochannels*. In SPIE BiOS, pp. 895008-895008. International Society for Optics and Photonics, 2014.
- (32) Xiaohua Huang, Manuel J. Gordon, and Richard N. Zare. *Current-monitoring method for measuring the electroosmotic flow rate in capillary zone electrophoresis*. Analytical Chemistry 60, no. 17 (1988): 1837-1838.
- (33) Neelesh A. Patankar, and Howard H. Hu. *Numerical simulation of electroosmotic flow*. Analytical Chemistry 70, no. 9 (1998): 1870-1881.
- (34) Norman J. Dovichi, and Jianzhong Zhang. *How capillary electrophoresis sequenced the human genome*. Angewandte Chemie International Edition 39, no. 24 (2000): 4463-4468.
- (35) Suman Chakraborty, and Amit Kumar Srivastava. *Generalized model for time periodic electroosmotic flows with overlapping electrical double layers*. Langmuir 23, no. 24 (2007): 12421-12428.
- (36) Kosmulski, Marek. *Chemical properties of material surfaces*. Vol. 102. CRC press, 2001.
- (37) Manish Keswani, Srini Raghavan, Pierre Deymier, and Steven Verhaverbeke. *Megasonic cleaning of wafers in electrolyte solutions: Possible role of electro-acoustic and cavitation effects*. Microelectronic Engineering 86, no. 2 (2009): 132-139.
- (38) Hannes Risken, *Fokker-Planck Equation*. Springer Berlin Heidelberg, 1984.
- (39) Jörg Enderlein, David L. Robbins, W. Patrick Ambrose, and Richard A. Keller. *Molecular shot noise, burst size distribution, and single-molecule detection in fluid flow: effects of multiple occupancy*. The Journal Of Physical Chemistry A 102, no. 30 (1998): 6089-6094.
- (40) M. Kirchner, and M. Kahl. *Raith-Electron Beam Lithography for Research*. Acta Physica Polonica A 116, no. s (2009): s198-s200.

- (41) Michael Wahl, Hans-Juergen Rahn, Tino Roehlicke, Gerald Kell, Daniel Nettels, Frank Hillger, Ben Schuler, and Rainer Erdmann. *Scalable time-correlated photon counting system with multiple independent input channels*. Review of Scientific Instruments 79, no. 12 (2008): 123113.